


ORIGINAL ARTICLE

Blocking transferrin receptor inhibits the growth of lung adenocarcinoma cells in vitro

Yihe Wu¹, Jinming Xu¹, Jinbo Chen², Meirong Zou², Aizemaiti Rusidanmu¹ & Rong Yang³ 

1 Department of Thoracic Surgery, The First Affiliated Hospital, College of Medicine, Zhejiang University, Hangzhou, China

2 College of Medicine, Zhejiang University, Hangzhou, China

3 Department of Radiology, The First Affiliated Hospital, College of Medicine, Zhejiang University, Hangzhou, China

Keywords

Antibody blocking; cell proliferation; KRAS; lung adenocarcinoma; transferrin receptor.

Correspondence

Rong Yang, Department of Radiology, The First Affiliated Hospital, College of Medicine, Zhejiang University, No. 79 Qingchun Road, Hangzhou 310003, Zhejiang Province, China.
Tel: +86 571 8723 6399
Fax: +86 571 8723 6399
Email: dryangrong@zju.edu.cn

Received: 19 October 2017;

Accepted: 8 November 2017.

doi: 10.1111/1759-7714.12572

Thoracic Cancer 9 (2018) 253–261

Abstract

Background: Transferrin receptor (TfR) is expressed in most lung cancers and is an indicator of poor prognosis in certain groups of patients. In this study, we blocked cell surface TfR to inhibit lung adenocarcinoma (LAC) cell growth in vitro and investigated the associated molecular mechanisms to determine a potential therapeutic target in human LAC.

Methods: RNA interference and antibody blocking techniques were used to block the function of TfR in LAC cells, and cell proliferation assays were used to detect the results. Affymetrix microarray analysis was conducted using H1299 cells in which TfR was blocked with an antibody to investigate the molecular mechanisms involved.

Results: The cell proliferation assay demonstrated that H1299 cell proliferation was significantly inhibited after small interfering RNA knockdown or blocking of TfR. Mechanistic studies found that 100 genes were altered more than two-fold after TfR was blocked and that blocking TfR was accompanied by decreased expression of the oncogene *KRAS*.

Conclusion: Our data provide evidence that blocking TfR could significantly inhibit LAC proliferation by targeting the oncogene *KRAS*; therefore, TfR may be a therapeutic target for LAC. In addition, our results suggest a new method for blocking the signal from the oncogene *KRAS* by targeting TfR in LAC.

Introduction

Lung cancer remains the leading cause of cancer-related death worldwide. Non-small cell lung cancer (NSCLC) subtypes, including lung adenocarcinoma (LAC), account for approximately 85% of all lung cancers.¹ Although tremendous efforts have been devoted to improving treatment procedures through novel chemotherapies combined with targeted agents, the overall survival rate remains low.² Transferrin receptor (TfR) is a 190 kDa glycoprotein expressed on the cytoplasmic membrane of a wide variety of cells.^{3,4} One of its key roles is controlling cell growth through iron uptake. However, there is evidence that TfR has many other biological roles in addition to its primary function of facilitating iron transport and metabolism, such as its profound effect on mammalian cell growth and productivity.^{5,6} TfR expression is normally restricted to a limited number of sites in humans, including basal

keratinocytes of the epidermis; islet cells of the pancreas; and parenchymal cells of the liver, testis, and pituitary gland.^{7–9} In healthy lung tissue, airway and alveolar epithelia and bronchial glands do not express TfR.⁷ However, TfR is expressed in most lung cancers and the presence of TfR in NSCLCs is an indicator of poor prognosis in certain groups of patients.^{7,10} In the present study we blocked cell surface TfR with the aim of inhibiting LAC cell growth in vitro, and investigated the associated molecular mechanisms to find a potential therapeutic target in human LAC.

Methods

Cell culture

Normal human bronchial epithelial (HBE) cells and LAC cell lines (H1299 and A549) were purchased from

American Type Culture Collection (ATCC, Rockville, MD, USA). These cells were cultured in Dulbecco's Modified Eagle medium (DMEM; Corning, Christiansburg, VA, USA) supplemented with 10% fetal bovine serum and a 1% antibiotic mixture (100 U/mL penicillin G and 100 µg/mL streptomycin sulfate; Beyotime Biotechnology, Shanghai, China), and incubated at 37°C in a humidified 5% CO₂ atmosphere. Upon reaching 90% confluence, the cells were dissociated using 0.25% trypsin (HyClone, Shanghai, China) and subcultured.

Immunofluorescence staining

HBE, H1299, and A549 cells were harvested from flasks and washed with phosphate buffered saline. Each sample contained 100 000 cells and was resuspended in 10 µL of a 50-fold-diluted human Fc receptor binding inhibitor (eBioscience, San Diego, CA, USA) for 5 minutes on ice, followed by staining with 2 µL of either a phycoerythrin-labeled human TfR antibody (OKT9, eBioscience) or a PE-labeled mouse immunoglobulin G1 (IgG1) isotype control antibody (P3.6.2.8.1, eBioscience) for 30 minutes at 4°C in the dark. The cells were then washed three times and resuspended in 400 µL of ice-cold phosphate buffered saline/2 mM ethylene-diamine-tetraacetic acid. The median fluorescence intensity (MFI) of the samples was quantified using an Attune cytometer with a 488 nm excitation laser and a 574/26 nm emission filter (Life Technologies, Waltham, MA, USA). Cell populations were gated according to the forward and side scattering channel, and 10 000 events were collected. Data analysis was performed using Attune cytometer software (Life Technologies). Experiments were conducted three times.

RNA interference

A transfection mix consisting of 1 µL of RNAiMAX (Invitrogen, Carlsbad, CA, USA) and 12 nM TfR siRNA (Silencer Select small interfering RNAs [siRNAs] 107 046, 107 047, and 107 048) purchased from Ambion in Opti-Mem (Invitrogen) was mixed with suspended cells for 20 minutes at room temperature prior to seeding at 5000 cells per well in 96-well plates. The medium was changed to DMEM after 24 hours. Total cellular RNA was extracted using 1× Nucleic Acid Purification Lysis Solution (Applied Biosystems, Foster City, CA, USA).

Antibody blocking of transferrin receptor (TfR)

An antihuman TfR monoclonal antibody (M-A712) used for blocking was purchased from BD Biosciences Pharmingen (San Diego, CA, USA).¹¹ Cells were incubated with

25 µg/mL isotype control or the TfR antibodies.¹¹ After 24, 48, 72, and 96 hours, cellular RNA was harvested using 1× Nucleic Acid Purification Lysis Solution (Applied Biosystems).

Proliferation assay

Cell proliferation was measured using colorimetric 3-(4,5-dimethylthiazol-2-yl)-5-(3-carboxymethoxyphenyl)-2-(4-sulfophenyl)-2H-tetrazolium, inner salt (MTS) assay (CellTiter 96 AQueous One Solution Cell Proliferation Assay; Promega, Madison, WI, USA). H1299 cells (2×10^4 cells/mL) were incubated with 25 µg/mL anti-TfR antibody in complete medium at 37°C and 5% CO₂. The proliferation assay was performed at 24, 48, 72, and 96 hours after antibody blocking. The MTS assay was performed as previously described.¹² Each experiment was performed three times, and the typical results are shown.

Microarray analysis

Cellular RNA from H1299 cells was extracted using TRIzol (Invitrogen), and quality control was performed as directed by the Affymetrix expression technical manual. RNA (50 ng) was used to produce biotin-labeled complementary RNA, which was hybridized to the Affymetrix GeneChip Human Genome U133 Plus 2.0 array (Affymetrix, Inc., Santa Clara, CA, USA). Array washing, scanning, and probe quantification protocols were performed according to the manufacturer's instructions using Affymetrix GeneChip Operating Software (GCOS) (<http://www.affymetrix.com>).¹³ Genes that displayed two-fold or greater expression changes between the control and antibody blocking groups were filtered using the Student's *t*-test with a significance threshold of $P < 0.05$. Hierarchical clustering with average linkage was performed only for the differentially expressed genes (DEGs), using Cluster 3.0. The cluster data were visualized using Java TreeView software (Microsoft, Redmond, WA, USA). Gene ontology (GO) and pathway analysis of the DEGs were performed using CapitalBio Molecule Annotation System (MAS) version 3.0 (<http://bioinfo.capitalbio.com/mas3/>), which can integrate multiple biological databases with the MAS core database. The information required for pathway analysis was obtained from three pathway databases, the Kyoto Encyclopedia of Genes and Genomes (KEGG), Biocarta, and GenMAPP, which are the major authoritative pathway databases.¹²

Real-time PCR

Total RNA was extracted and then reverse transcribed into complementary DNA (cDNA) using a PrimeScript RT reagent kit (TaKaRa Biotechnology, Dalian, China) according

to the manufacturer's instructions. The PCR reactions were carried out in a 50- μ L reaction mixture with a 96-well format using SYBR Premix Ex Taq II (TaKaRa Biotechnology) in a 7300 real-time PCR system (Applied Biosystems). Three biological replicates were created for each gene. The results were normalized to glyceraldehyde 3-phosphate dehydrogenase (GAPDH), and the amount of each transcript was calculated using the formula $2^{-(\Delta CT(\text{target gene}) - \Delta CT(\text{GAPDH}))}$, where the cycle threshold value indicates the time at which the fluorescence rose appreciably above the background fluorescence.¹⁴ The following primers were used: Tfr, 5'-CA GCCAGCAGAAGCATT-3' and 5'-CCAAGAACCGCTT-TATCCAG-3'; KRAS, 5'-GACTGAATATAAACTTGTGG-TAGTTGGACCT-3' and 5'-TCCTCTTGACCTGCTGTGT CG-3'; and GAPDH, 5'-CAAGATCATCAGCAATGCCT-3' and 5'-AGGGATGATGTTCTGGAGAG-3'.

Western blot

Total cellular proteins were isolated from cultured cells using lysis buffer and assayed by Western blot according to previously described procedures.¹⁵ Proteins were detected according to the manufacturer's instructions. Briefly, equal amounts of protein were denatured, electrophoresed (SDS-PAGE gel kit, Beyotime), and transferred to polyvinylidene fluoride membranes (Millipore, Billerica, MA, USA). The membranes were then incubated overnight with primary antibody, washed with tris-buffered saline plus tween 20, and then incubated with a second antibody. The proteins were detected using ECL chemiluminescence (Millipore). The primary antibodies were mouse anti-Tfr (1:1000, M-A712, BD Pharmingen), and mouse anti-KRAS (1:1000) and mouse anti-GAPDH (1:1000; Cell Signaling Technology, Danvers, MA, USA). The secondary antibody was horseradish peroxidase-conjugated rabbit anti-mouse IgG (1:10 000; Cell Signaling Technology).

Statistical analysis

The results are presented as the mean \pm standard deviation. Proliferation assay and real-time PCR data were analyzed using paired *t*-tests. Statistical analysis was conducted using SPSS version 13.0 statistical software (SPSS Inc., Chicago, IL, USA). A two-tailed *P* value of < 0.05 was considered statistically significant.

Results

Tfr expression

The Tfr expression levels in the normal HBE cells and lung adenocarcinoma cell lines (H1299 and A549) were

measured via flow cytometry. The cells were immunostained with a fluorescent-labeled anti-Tfr antibody or an isotype control antibody. As shown in Figure 1a, the MFI across three cell lines was unchanged when stained with the isotype antibody, indicating that little fluorescence was caused by non-specific antibody binding. By contrast, H1299 and A549 cells demonstrated a significantly higher MFI after being stained with the anti-Tfr antibody compared to the HBE cells and the MFI in H1299 cells was higher than in A549 cells (Fig 1a). Similarly, H1299 and A549 cells demonstrated markedly higher levels of Tfr protein expression compared to the HBE cell line, as determined by Western blot analysis (Fig 1b). Additionally, the Tfr protein expression level in H1299 cells was higher than in A549 cells (Fig 1b). Therefore, the H1299 cells were considered the Tfr overexpressing cell model for our study.

Tfr knockdown using small interfering RNA inhibits H1299 cell proliferation

As an initial experiment to determine whether Tfr is functionally involved in H1299 cell proliferation, we assessed the effect of Tfr knockdown. H1299 cells were transfected with an irrelevant control siRNA or a Tfr-specific siRNA 24 hours after cells were seeded. Real-time PCR confirmed the knockdown efficiency of the Tfr-siRNA. Tfr messenger RNA (mRNA) expression was significantly decreased ($P = 0.004$ vs. the negative control; $P = 0.009$ vs. the mock transfection) (Fig 1c) 96 hours after transfection in H1299 cells following the silencing of Tfr by its specific siRNA, resulting in downregulation of the Tfr protein (Fig 1d).

After transfection, the cells were incubated in complete medium for an additional 24, 48, 72, or 96 hours. MTS assay results showed that transfection with the Tfr siRNA resulted in significantly decreased cell viability compared to the negative control at each time point (Fig 2a).

Blocking cell surface Tfr inhibits H1299 cell proliferation

Because Tfr knockdown appeared to inhibit H1299 cell proliferation, we investigated whether blocking surface Tfr had a similar effect. Initially, we performed blocking experiments in which antibodies were added to the cells 24 hours after cell seeding. H1299 cells were incubated with irrelevant mouse IgG negative control or the anti-Tfr. The cells were then incubated in complete medium for an additional 24, 48, 72, or 96 hours. MTS assay results showed that blocking Tfr also resulted in significantly decreased cell viability compared to the negative control at each time point (Fig 2b).

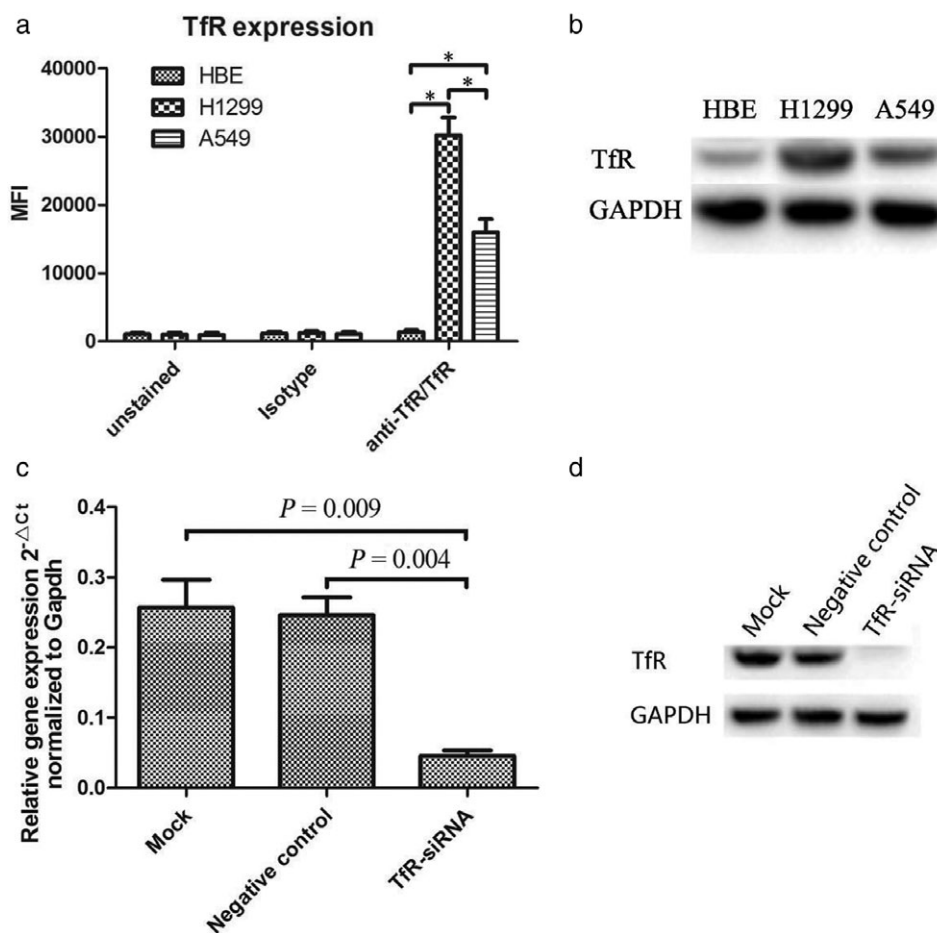


Figure 1 Transferrin receptor (TfR) protein expression in human bronchial epithelial (HBE), H1299, and A549 cells and effect of TfR small interfering RNA (siRNA) in H1299 cells. **(a)** HBE, H1299, and A549 cells were immunostained with the anti-TfR antibody, which binds to TfR, and by an isotype antibody, which served as a non-specific binding control. Median fluorescence intensity (MFI) was quantified via flow cytometry. Data are representative of at least three independent experiments. (Data points indicate mean ± standard deviation; * $P < 0.05$). **(b)** Western blot analysis of TfR protein expression in HBE, H1299, and A549 cells. Glyceraldehyde 3-phosphate dehydrogenase (GAPDH) was used as a loading control. **(c)** Effect of TfR siRNA on the TfR messenger RNA level in H1299 cells, determined by real-time PCR. The messenger RNA levels were significantly decreased following the siRNA-mediated knockdown of TfR compared to the negative control ($P = 0.004$) and mock-transfected ($P = 0.009$) cells. **(d)** TfR protein levels in the TfR-knockdown H1299 cells, as determined by Western blot. GAPDH was used as a loading control. Mock group: untreated; negative control group: transfected with control siRNA; TfR siRNA group: transfected with a TfR-specific siRNA.

Differentially expressed genes

To investigate the molecular mechanisms of blocking TfR inhibiting cell proliferation, cDNA microarray analysis was utilized to identify regulated gene expression 72 hours after TfR was blocked. A total of six microarrays were used, and three biological replicates were created for each condition (anti-TfR vs. the negative control group). Transcriptome analysis between the negative control and anti-TfR groups revealed that 100 DEGs with a cut-off threshold of 2 ($P < 0.05$) showed a correct hybridization signal on the six arrays. Of the 100 differentially expressed mRNAs between the negative control and anti-TfR groups, 4 (4.0%) were highly expressed in the anti-TfR groups and 96 (96.0%) were

highly expressed in the negative control group. Hierarchical clustering is presented in Figure 2c.

GO analysis of the 100 DEGs revealed that blocking TfR regulates genes that are involved in cell proliferation, apoptosis, cell cycle, transcription, translation, biosynthetic processes, metabolic processes, protein and nucleic acid binding, proteolysis, signal transduction, and ion transmembrane transport regulation, among others (Table S1). Table 1 shows the DEGs associated with cell proliferation, apoptosis, the cell cycle, and transcription. Pathway analysis was successfully performed to associate differentially regulated genes with known specific biological pathways using the CapitalBio MAS platform. This pathway analysis revealed the central regulatory role played by *KRAS* (Fig 3).

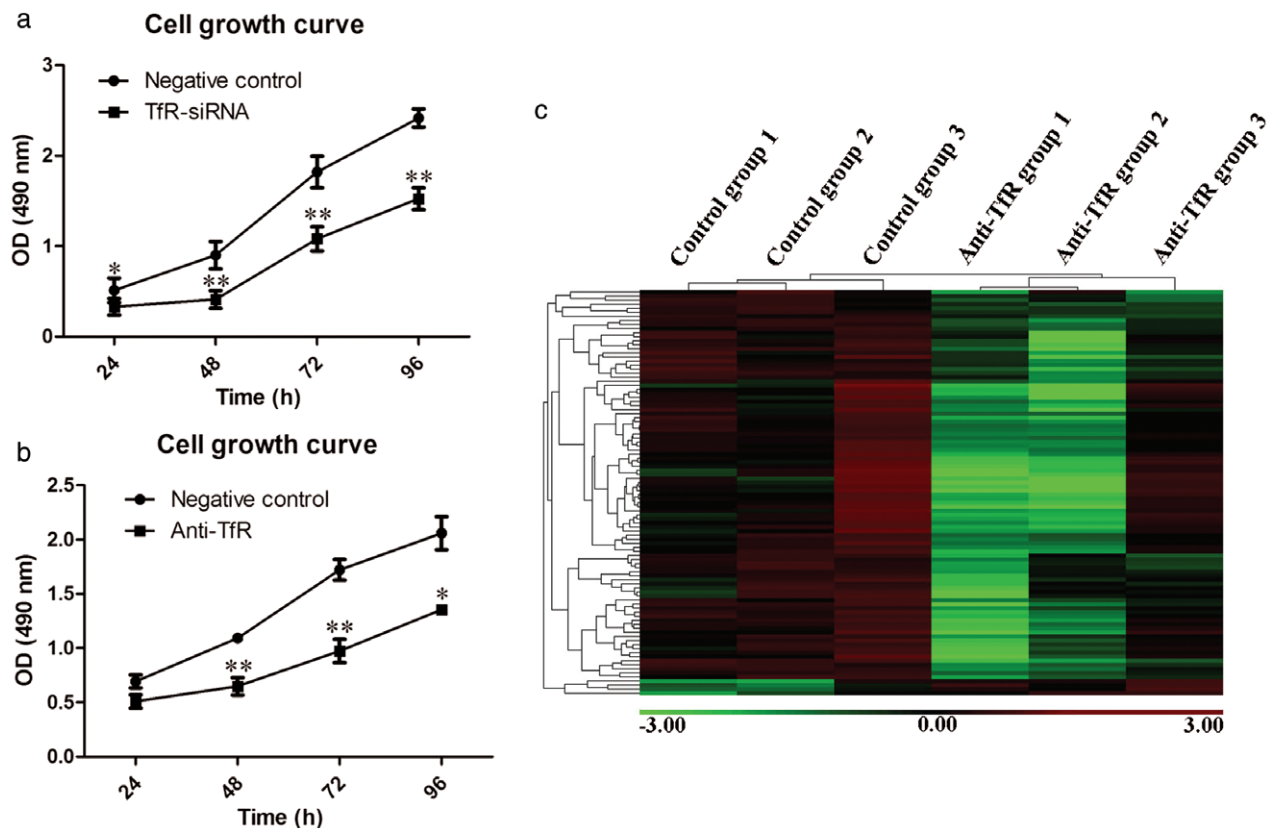


Figure 2 The effect of transferrin receptor (TfR) small interfering RNA (siRNA) or TfR antibody blocking on cell proliferation and Heat map of the 100 overlapping genes. Effects of (a) TfR siRNA and (b) blocking cell surface TfR on cell proliferation, determined by MTS assay. * $P < 0.05$ versus the negative control; ** $P < 0.01$ versus the negative control. OD, optical density. (c) Hierarchical clustering of 100 messenger RNA expression patterns in the anti-TfR versus the negative control group. Red/green indicates an increase/decrease in gene expression, relative to the universal mean for each gene.

Validation of microarray data by real-time PCR and Western blot

To validate the microarray results, we performed real-time PCR and Western blot analysis on the negative control and anti-TfR H1299 cells. *KRAS* was relevant to the biological function of proliferation and could partially illuminate the molecular mechanisms of cell proliferation induced by blocking TfR (Table 1). Because the pathway analysis showed that *KRAS* plays a central regulatory role after TfR is blocked (Fig 3), *KRAS* was selected for further analysis. To observe the dynamic trend of the *KRAS* gene after blocking TfR, we performed real-time PCR on control and anti-TfR H1299 cells 24, 48, 72, and 96 hours after blocking TfR. The results were analyzed by comparing relative gene expression using the $2^{-\Delta C_t}$ method.¹⁴ *KRAS* mRNA expression levels in the anti-TfR group were significantly lower than in the negative control from 24 to 96 hours after blocking ($P < 0.05$) (Fig 4a). We then determined whether blocking TfR affected the expression of endogenous *KRAS* at the translational level. As shown in

Figure 4b, Western blot analysis revealed that the level of *KRAS* protein expression in the anti-TfR group was significantly inhibited compared to that in the negative control group 96 hours after blocking.

Discussion

Transferrin receptor is a membrane protein expressed at low levels in most cells and can bind to the iron transport glycoprotein Tf, which consequently triggers fast internalization.^{16–19} Our investigation of the functions and properties of TfR in iron transport indicate that TfR plays a greater biological role than previously thought.^{5,20,21} Xie *et al.* reported that H1299 cells demonstrate significantly higher TfR expression compared to A549 and H460 cells.²² Therefore, we chose to use A549 and H1299 cell lines to locate a TfR overexpressing cell. In this study, we observed upregulated protein levels of cellular TfR in lung adenocarcinoma H1299 cells (Fig 1a,b). After siRNA knockdown or TfR blocking, we observed inhibition of H1299 cell

Table 1 Genes associated with proliferation, apoptosis, cell cycle, and transcription

Function	Gene ID	Gene title	Gene symbol	Fold change (Anti-TfR vs. control groups)	P
Proliferation	8678	Beclin 1, autophagy related	BECN1	0.4585	0.0006
	1296	Collagen, type VIII, alpha 2	COL8A2	0.3775	0.0437
	2100	Estrogen receptor 2 (ER beta)	ESR2	0.3821	0.0053
	3845	<i>Kirsten rat sarcoma viral oncogene homolog</i>	KRAS	0.4682	0.0053
	5697	Peptide YY	PYY	0.4656	0.0424
	9481	Solute carrier family 25, member 27	SLC25A27	0.3886	0.0392
Apoptosis	23 604	Death-associated protein kinase 2	DAPK2	0.4978	0.0199
Cell cycle	3537	Cytoskeleton associated protein 2	CKAP2	0.4244	0.0160
	54 737	M-phase phosphoprotein 8	MPHOSPH8	2.1859	0.0297
Transcription	4772	Nuclear factor of activated T-cells, cytoplasmic, calcineurin-dependent 1	NFATC1	0.4236	0.0018
	126 520	Polo-like kinase 5	PLK5	0.4779	0.0004
	5933	Retinoblastoma-like 1	RBL1	0.4931	0.0361
	6714	SRC proto-oncogene, non-receptor tyrosine kinase	SRC	0.3405	0.0157
	1386	Activating transcription factor 2	ATF2	0.4413	0.0174
	2303	Forkhead box C2 (MFH-1, mesenchyme forkhead 1)	FOXC2	0.4735	0.0075
	136 259	Kruppel-like factor 14	KLF14	0.4533	0.0070
	7849	Paired box 8	PAX8	0.4337	0.0344
	862	Runt-related transcription factor 1; translocated to, 1 (cyclin D-related)	RUNX1T1	0.3855	0.0130
	147 949	Zinc finger protein 583	ZNF583	0.4020	0.0107

proliferation, demonstrating that TfR plays a role in LAC growth (Fig 2a,b). Mechanistic studies suggest that blocking TfR may exert an effect by inhibiting *KRAS* (Figs 3, 4).

Transferrin receptor plays a crucial role in the cellular uptake of iron, and cellular iron deficiency arrests cell growth, leading to cell death.²³ TfR is expressed more abundantly in malignant tissues than in normal tissues because cancer cells require copious amounts of iron to maintain their high proliferation rates.²⁴ Therefore, TfR is an attractive target for immunotherapy and for the delivery of cytotoxic agents because of its increased expression in malignant compared to normal cells.^{25–27} TfR is expressed in most lung cancers, and the presence of TfR in NSCLCs may be an indicator of poor prognosis in certain groups of patients.⁷ Herein, we showed that TfR itself could possibly be a therapeutic target for LAC, with the anti-human TfR-specific antibody described in this manuscript. The mechanism behind the selective cancer cell killing ability of the anti-TfR antibody has not yet been elucidated. However, it is speculated that cancer cells require more iron than normal cells to sustain their abnormally rapid growth rates, thus reducing the intracellular iron concentration by preventing TfR-mediated cellular iron uptake may cause growth inhibition and cell death in cancer cells.^{28,29} In LAC, the anti-TfR antibody is suspected to block the internalization of transferrin into cancer cells, and the resulting transferrin deficiency might block the cell cycle and/or induce apoptotic cell death because of the potentially abnormal transferrin requirements of cancer cells. In

addition, Tf, which is the ligand for TfR, can act as a growth factor in most cells in tissue culture, as a neurotrophic factor during neural stem cell development, and as an angiogenic factor to promote endothelial cell migration.⁵ Blocking TfR results in the inhibition of these Tf functions. In this study, we observed that the proliferation of H1299 cells was significantly inhibited after siRNA knockdown or after TfR was blocked (Fig 2a,b). These results indicate that TfR is potentially a therapeutic target for lung adenocarcinoma. In addition, the small-molecule iron transport inhibitor ferristatin/NSC306711 promotes TfR degradation, which may be used in LAC therapy in the future.^{17,30}

As previously reported, TfR expression is significantly upregulated in cancer, increasing several 100-fold in various tumor cell lines and malignant tissues.²⁶ Although the receptor has an established physiological function within the tissue, its aberrant stimulation and overexpression in cancer could act as an attractive targeting molecule for cancer therapy. A number of studies have shown the capacity of anti-transferrin receptor antibodies to limit cell growth in cultured, normal, and malignant cells.²⁶ However, no relevant study has reported whether blocking TfR will have any adverse effects on other normal tissues or organs. This issue requires further exploration in future research.

Complementary DNA microarray analysis showed that 100 genes were altered more than two-fold after TfR was blocked. We grouped the 100 regulated genes into

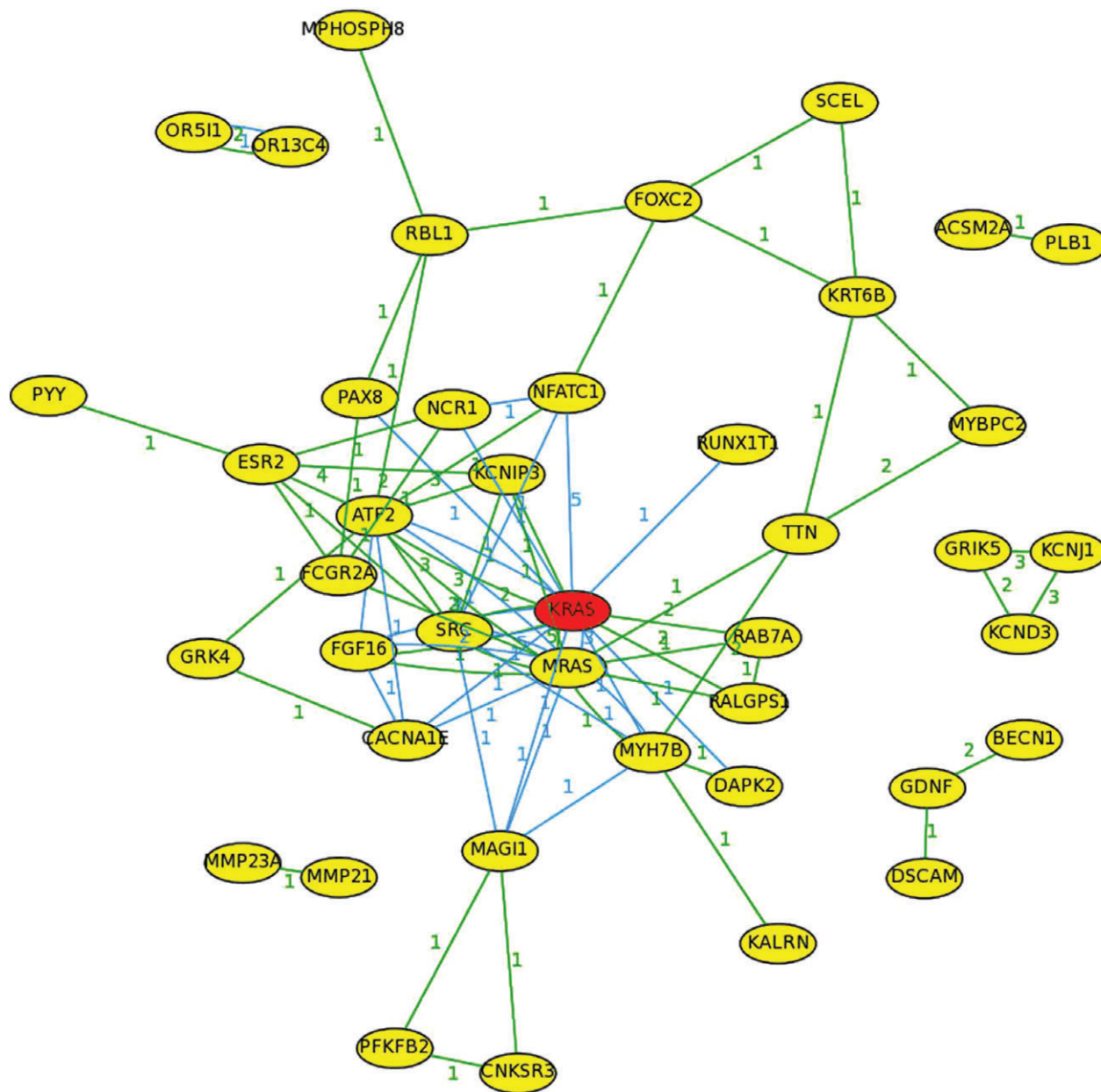


Figure 3 The differentially expressed genes were analyzed using CapitalBio MAS version 3.0. The blue lines indicate that the information regarding the gene relationships was obtained from the KEGG database, and the green lines indicate that the information was obtained from the GenMAPP database. Pathway analysis revealed that *KRAS* (colored red) has a greater number of connections with other genes.

functional categories that included cell proliferation, apoptosis, cell cycle, transcription, translation, biosynthetic processes, metabolic processes, protein and nucleic acid binding, proteolysis, signal transduction, and ion transmembrane transport regulation, among others (Table S1). Pathway analysis showed that *KRAS* plays a central regulatory role, and was thus selected for further analysis (Fig 3). Real-time PCR and Western blot analysis validated the array findings for the *KRAS* gene (Fig 4).

KRAS is an oncogene that functions as a critical molecular switch for various biological processes, including cell proliferation, survival, differentiation, and death.^{31–33} *KRAS* is associated with increased cell growth and differentiation in many cancers.^{34–36} In addition, Yoon *et al.* showed that *KRAS* plays a key role in signal transduction in NSCLC.³⁷ Activating *KRAS* mutations are present in more than 80% of all NSCLCs.^{38,39} This mutation leads to constant receptor phosphorylation and

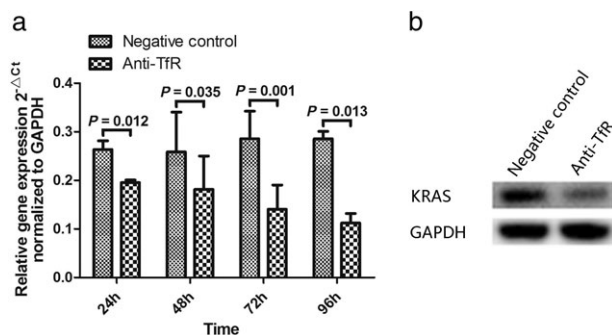


Figure 4 (a) Validation of *KRAS* messenger RNA (mRNA) expression using real-time PCR. Comparison of the dynamic trend of mRNA expression of *KRAS* in the negative control and anti-TfR groups 24, 48, 72, and 96 hours after TfR was blocked. Data analysis using the $2^{-\Delta\Delta Ct}$ method shows the relative expression levels of individual genes when normalized to the internal control, glyceraldehyde 3-phosphate dehydrogenase (GAPDH). (b) Validation of protein expression using Western blot. *KRAS* protein levels were examined in the negative control and anti-TfR groups 96 hours after TfR was blocked. GAPDH was used as a loading control. Negative control group: H1299 cells were incubated with an irrelevant mouse immunoglobulin G (IgG) antibody; anti-TfR group: cells were incubated with an anti-TfR antibody.

the activation of downstream cascade pathways (such as the RAS, PI3K, and AKT signaling pathways) that are important for the regulation of cell proliferation and growth.⁴⁰ It has been shown that activating *KRAS* mutations lead to subsequent activation of the RAS–RAF pathway.⁴⁰ Inhibiting *KRAS* results in the inhibition of cancer cell proliferation and growth; however, direct *KRAS* targeting has proven to be difficult.^{41–43} Some strategies for interrupting oncogenic *KRAS* signals, such as inhibiting post-translational modification and Ras protein membrane association, have been employed, but unfortunately no clinical benefits using these methods have been determined.⁴¹ In this study, we observed that blocking TfR resulted in the downregulation of *KRAS* mRNA and protein levels in lung adenocarcinoma H1299 cells (Figs 3, 4). Our results suggest a new method for blocking the oncogenic *KRAS* signal by targeting TfR in LAC. The mechanisms of TfR suppression of *KRAS* expression are unknown. TfR acts as a growth factor in most cells in tissue culture,^{5,6} thus we hypothesize that this may be related to the non-facilitating iron transport of TfR and intend to conduct further research.

In conclusion, we found that blocking TfR could significantly inhibit LAC proliferation by targeting the oncogene *KRAS*. These results indicate that blocking TfR may suppress LAC progression and imply its potential application in LAC therapy. We plan to initiate a clinical trial to determine the usefulness and benefits of TfR as a therapeutic target for LAC.

Acknowledgments

This work was supported by the National Natural Science Foundation of China (81441079, 31700690) and the Projects of Medical and Health Technology Program in Zhejiang province (2014KYB094).

Disclosure

No authors report any conflict of interest.

References

- Liang W, Zhang L, Jiang G *et al*. Development and validation of a nomogram for predicting survival in patients with resected non-small-cell lung cancer. *J Clin Oncol* 2015; **33**: 861–9.
- Xue W, Dahlman JE, Tammela T *et al*. Small RNA combination therapy for lung cancer. *Proc Natl Acad Sci U S A* 2014; **111**: E3553–61.
- Liu Y, Tao J, Li Y *et al*. Targeting hypoxia-inducible factor-1alpha with Tf-PEI-shRNA complex via transferrin receptor-mediated endocytosis inhibits melanoma growth. *Mol Ther* 2009; **17**: 269–77.
- Johnsen KB, Moos T. Revisiting nanoparticle technology for blood-brain barrier transport: Unfolding at the endothelial gate improves the fate of transferrin receptor-targeted liposomes. *J Control Release* 2016; **222**: 32–46.
- Brandsma ME, Jevnikar AM, Ma S. Recombinant human transferrin: Beyond iron binding and transport. *Biotechnol Adv* 2011; **29**: 230–8.
- Wei W, Wu Y, Ying Y, Li S, Hu S, Zhang H. Role of augmented transferrin during the retraining for undeveloped left ventricle. *J Cell Mol Med* 2015; **19**: 2423–31.
- Whitney JF, Clark JM, Griffin TW, Gautam S, Leslie KO. Transferrin receptor expression in nonsmall cell lung cancer. Histopathologic and clinical correlates. *Cancer* 1995; **76**: 20–5.
- Kindrat I, Tryndyak V, de Conti A *et al*. MicroRNA-152-mediated dysregulation of hepatic transferrin receptor 1 in liver carcinogenesis. *Oncotarget* 2016; **7**: 1276–87.
- Habashy HO, Powe DG, Staka CM *et al*. Transferrin receptor (CD71) is a marker of poor prognosis in breast cancer and can predict response to tamoxifen. *Breast Cancer Res Treat* 2010; **119**: 283–93.
- Dowlati A, Loo M, Bury T, Fillet G, Beguin Y. Soluble and cell-associated transferrin receptor in lung cancer. *Br J Cancer* 1997; **75**: 1802–6.
- Martin DN, Uprichard SL. Identification of transferrin receptor 1 as a hepatitis C virus entry factor. *Proc Natl Acad Sci U S A* 2013; **110**: 10777–82.
- Wu YH, Wang J, Gong DX, Gu HY, Hu SS, Zhang H. Effects of low-level laser irradiation on mesenchymal stem cell proliferation: A microarray analysis. *Lasers Med Sci* 2012; **27**: 509–19.
- Wang L, Xu J, Zhao C, Zhao L, Feng B. Antiproliferative, cell-cycle dysregulation effects of novel asiatic acid

- derivatives on human non-small cell lung cancer cells. *Chem Pharm Bull (Tokyo)* 2013; **61**: 1015–23.
- 14 Xu H, Han Y, Liu B, Li R. Unc-5 homolog B (UNC5B) is one of the key downstream targets of N-alpha-Acetyltransferase 10 (Naa10). *Sci Rep* 2016; **6**: 38508.
 - 15 Wu Y, Feng W, Zhang H *et al.* Ca²⁺-regulatory proteins in cardiomyocytes from the right ventricle in children with congenital heart disease. *J Transl Med* 2012; **10**: 67.
 - 16 Xie Y, Kim NH, Nadiathe V *et al.* Targeted delivery of siRNA to activated T cells via transferrin-polyethylenimine (Tf-PEI) as a potential therapy of asthma. *J Control Release* 2016; **229**: 120–9.
 - 17 Horonchik L, Wessling-Resnick M. The small-molecule iron transport inhibitor ferristatin/NSC306711 promotes degradation of the transferrin receptor. *Chem Biol* 2008; **15**: 647–53.
 - 18 Liu K, Lei R, Li Q *et al.* Transferrin receptor controls AMPA receptor trafficking efficiency and synaptic plasticity. *Sci Rep* 2016; **6**: 21019.
 - 19 Wang B, Zhang J, Song F *et al.* EGFR regulates iron homeostasis to promote cancer growth through redistribution of transferrin receptor 1. *Cancer Lett* 2016; **381**: 331–40.
 - 20 Mizutani T, Ishizaka A, Nihei C. Transferrin receptor 1 facilitates poliovirus permeation of mouse brain capillary endothelial cells. *J Biol Chem* 2016; **291**: 2829–36.
 - 21 Ross SR, Schofield JJ, Farr CJ, Bucan M. Mouse transferrin receptor 1 is the cell entry receptor for mouse mammary tumor virus. *Proc Natl Acad Sci U S A* 2002; **99**: 12386–90.
 - 22 Xie Y, Killinger B, Moszczynska A, Merkel OM. Targeted delivery of siRNA to transferrin receptor overexpressing tumor cells via peptide modified polyethylenimine. *Molecules* 2016; **21**: pii: E1334.
 - 23 Kasibhatla S, Jessen KA, Maliartchouk S *et al.* A role for transferrin receptor in triggering apoptosis when targeted with gambogic acid. *Proc Natl Acad Sci U S A* 2005; **102**: 12095–100.
 - 24 Nagai K, Nakahata S, Shimosaki S *et al.* Development of a complete human anti-human transferrin receptor C antibody as a novel marker of oral dysplasia and oral cancer. *Cancer Med* 2014; **3**: 1085–99.
 - 25 Daniels-Wells TR, Penichet ML. Transferrin receptor 1: A target for antibody-mediated cancer therapy. *Immunotherapy* 2016; **8**: 991–4.
 - 26 Tortorella S, Karagiannis TC. Transferrin receptor-mediated endocytosis: A useful target for cancer therapy. *J Membr Biol* 2014; **247**: 291–307.
 - 27 Dufès C, Al Robaian M, Somani S. Transferrin and the transferrin receptor for the targeted delivery of therapeutic agents to the brain and cancer cells. *Ther Deliv* 2013; **4**: 629–40.
 - 28 Kukulj S, Jaganjac M, Boranic M, Krizanac S, Santic Z, Poljak-Blazi M. Altered iron metabolism, inflammation, transferrin receptors, and ferritin expression in non-small-cell lung cancer. *Med Oncol* 2010; **27**: 268–77.
 - 29 Prutki M, Poljak-Blazi M, Jakopovic M, Tomas D, Stipanec I, Zarkovic N. Altered iron metabolism, transferrin receptor 1 and ferritin in patients with colon cancer. *Cancer Lett* 2006; **238**: 188–96.
 - 30 Byrne SL, Buckett PD, Kim J *et al.* Ferristatin II promotes degradation of transferrin receptor-1 in vitro and in vivo. *PLoS One* 2013; **8**: e70199.
 - 31 Rajalingam K, Schreck R, Rapp UR, Albert S. Ras oncogenes and their downstream targets. *Biochim Biophys Acta* 2007; **1773**: 1177–95.
 - 32 Mou H, Moore J, Malonia SK *et al.* Genetic disruption of oncogenic Kras sensitizes lung cancer cells to Fas receptor-mediated apoptosis. *Proc Natl Acad Sci U S A* 2017; **114**: 3648–53.
 - 33 Tape CJ, Ling S, Dimitriadi M *et al.* Oncogenic KRAS regulates tumor cell signaling via stromal reciprocation. (Published erratum appears in Cell 2016; 165: 1818.). *Cell* 2016; **165**: 910–20.
 - 34 Friday BB, Adjei AA. K-ras as a target for cancer therapy. *Biochim Biophys Acta* 2005; **1756**: 127–44.
 - 35 Arvanitakis M, Van Laethem JL, Parma J, De Maertelaer V, Delhaye M, Devière J. Predictive factors for pancreatic cancer in patients with chronic pancreatitis in association with K-ras gene mutation. *Endoscopy* 2004; **36**: 535–42.
 - 36 Zorde Khvalevsky E, Gabai R, Rachmut IH *et al.* Mutant KRAS is a druggable target for pancreatic cancer. *Proc Natl Acad Sci U S A* 2013; **110**: 20723–8.
 - 37 Yoon YK, Kim HP, Han SW *et al.* KRAS mutant lung cancer cells are differentially responsive to MEK inhibitor due to AKT or STAT3 activation: Implication for combinatorial approach. *Mol Carcinog* 2010; **49**: 353–62.
 - 38 Shimamura T, Chen Z, Soucheray M *et al.* Efficacy of BET bromodomain inhibition in Kras-mutant non-small cell lung cancer. *Clin Cancer Res* 2013; **19**: 6183–92.
 - 39 Pan W, Yang Y, Zhu H, Zhang Y, Zhou R, Sun X. KRAS mutation is a weak, but valid predictor for poor prognosis and treatment outcomes in NSCLC: A meta-analysis of 41 studies. *Oncotarget* 2016; **7**: 8373–88.
 - 40 Wang ZD, Wei SQ, Wang QY. Targeting oncogenic KRAS in non-small cell lung cancer cells by phenformin inhibits growth and angiogenesis. *Am J Cancer Res* 2015; **5**: 3339–49.
 - 41 Mortazavi F, Lu J, Phan R *et al.* Significance of KRAS/PAK1/Crk pathway in non-small cell lung cancer oncogenesis. *BMC Cancer* 2015; **15**: 381.
 - 42 Lito P, Solomon M, Li LS, Hansen R, Rosen N. Allele-specific inhibitors inactivate mutant KRAS G12C by a trapping mechanism. *Science* 2016; **351**: 604–8.
 - 43 Manchado E, Weissmueller S, Morris JP IV *et al.* A combinatorial strategy for treating KRAS-mutant lung cancer. *Nature* 2016; **534**: 647–51.

Supporting Information

Additional Supporting Information may be found in the online version of this article at the publisher's website:

Table S1 Genes associated with various functions.